Asian Journal of Chemistry; Vol. 38, No. 6 (2026), 1619-1628
ASIAN JOURNAL OF CHEMISTRY
https://doi.org/10.14233/ajchem.2026.35912

Design, Synthesis, Molecular Docking Studies and Biological Evaluation of Novel Imidazole–1,2,3-Triazole Hybrid Derivatives as Anticancer and Antimicrobial Agents

POTHARAJU SUNIL KUMAR, RAMBABU BHUKYA, GOLI J. RUPASREE, NAMPALLY RAJITHA, NALAPARAJU NAGARAJU and RAMCHANDER JADHAV*

Department of Chemistry, University College of Science, Osmania University, Hyderabad-500007, India

*Corresponding author: E-mail: ramorgchemou@gmail.com

Received: 9 March 2026 *Accepted*: 21 May 2026 *Published online*: 31 May 2026 AJC-22389

The development of multifunctional heterocyclic hybrids offers a promising strategy for novel therapeutic discovery. In this study, a series of imidazole–triazole derivatives incorporating a 6-nitrobenzo[*d*][1,3]dioxole moiety were designed and synthesised and their structures were confirmed by IR, NMR and mass spectrometry. The synthesised compounds were evaluated for anticancer activity against MCF-7 cells, cytotoxicity toward NIH/3T3 normal cells and antimicrobial activity against selected strains. Among them, compound **6f** displayed the highest cytotoxic potency, while compounds **6d**, **6e** and **6i** also demonstrated significant activity. Structure–activity relationship studies indicated that both electronic and steric properties of substituents strongly influence biological activity, with electron-withdrawing groups generally enhancing anticancer potency. Molecular docking studies against the EGFR tyrosine kinase domain (PDB ID: 6LUD) revealed favourable ligand–protein interactions and compound **6f** exhibited the highest binding affinity with a docking score of -9.4 kcal/mol and hydrogen bond interaction with SER797. The docking protocol was validated with an RMSD value of 1.12 Å using the co-crystallised ligand osimertinib. The obtained results suggest that these imidazole–triazole hybrids may serve as promising lead molecules for further optimisation and biological investigation as potential anticancer agents.

Keywords: Imidazole-triazole hybrids, Debus-Radziszewski reaction, Molecular docking, Anticancer activity, Antimicrobial activity.

INTRODUCTION

Heterocyclic compounds represent a fundamental class of bioactive molecules extensively utilised in pharmaceutical sciences because of their remarkable structural diversity and broad range of pharmacological activities [1,2]. In particular, nitrogen-containing heterocycles have attracted significant scientific interest owing to their ability to interact efficiently with various biological targets involved in disease progression [3,4]. Among them, imidazole derivatives constitute an important pharmacophore in medicinal chemistry and have been widely reported for their anti-inflammatory, anticancer, antiviral, antimicrobial and antifungal properties [5-7]. The imidazole nucleus is capable of forming hydrogen bonding and π-π interactions with biomacromolecules, thereby contributing to enhanced biological activity. Several imidazole-containing compounds have demonstrated the ability to inhibit enzymes and receptors associated with tumor growth and cellular proliferation, making this scaffold highly valuable for anticancer drug development [8,9].

Similarly, triazole derivatives have emerged as important heterocyclic motifs in drug design due to their excellent pharmacokinetic and pharmacodynamic characteristics. The triazole ring possesses high metabolic stability, strong dipole moment and significant hydrogen-bonding capability, which facilitate effective interactions with biological targets [10,11]. Furthermore, triazole-containing compounds often exhibit improved aqueous solubility, enhanced binding affinity and increased bioavailability. Owing to these favourable properties, the triazole pharmacophore has been successfully incorporated into several clinically approved therapeutic agents (Fig. 1) [12]. Recent studies have demonstrated that triazole derivatives exhibit diverse biological activities, particularly anticancer and antimicrobial effects, thereby highlighting their importance in medicinal chemistry research.

In recent years, molecular hybridisation has become an efficient and rational strategy for the development of multifunctional therapeutic agents. This approach involves the integration of two or more biologically active pharmacophoric units into a single molecular framework with the aim

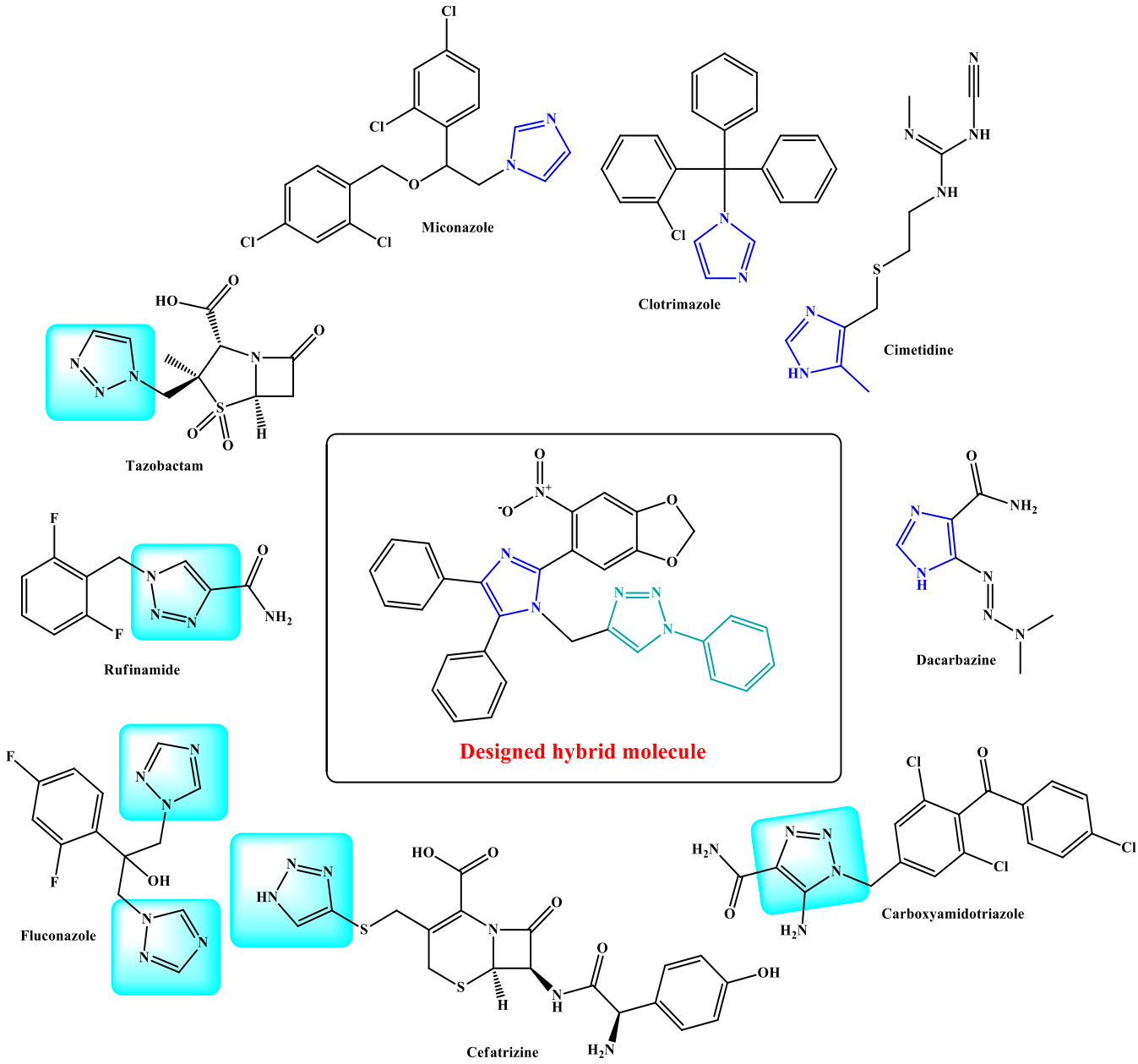

Fig. 1. Clinically approved drugs and designed hybrid molecules

of producing hybrid molecules possessing enhanced efficacy, improved selectivity and reduced toxicity [13-15]. Hybrid compounds frequently display synergistic biological effects due to the simultaneous contribution of multiple pharmacophoric moieties. In this regard, hybrid molecules containing both imidazole and triazole nuclei have shown considerable promise in the development of biologically active compounds, particularly in the fields of anticancer and antimicrobial drug discovery [16,17]. The combination of these two pharmacologically important heterocycles within a single scaffold may provide improved molecular interactions with biological targets and enhanced therapeutic potential.

Moreover, the incorporation of substituted aromatic systems into heterocyclic frameworks has been recognised as an effective strategy for modulating biological activity. Among these, nitrobenzodioxole derivatives have attracted attention due to their electron-deficient character and their ability to participate in strong intermolecular interactions with enzymes and receptor binding sites [18,19]. The presence of electron-withdrawing substituents can significantly influence the electronic distribution, lipophilicity and molecular recognition properties of bioactive compounds. Structure-activity relationship (SAR) investigations have revealed that such substitutions may contribute to enhanced pharmacological activity, improved target affinity and better selectivity toward biological systems [20].

Considering the significant biological importance of imidazole and triazole pharmacophores and the advantages associated with molecular hybridisation, the present investigation was undertaken to design and synthesize a new series of imidazole–triazole hybrid derivatives incorporating a 6-nitrobenzo[*d*][1,3]dioxole moiety. The synthesised compounds were

characterised using spectroscopic techniques and subsequently evaluated for their anticancer and antimicrobial activities. In addition, molecular docking studies were performed to investigate their possible binding interactions with selected biological targets and to explore their potential as promising therapeutic candidates [21-23].

EXPERIMENTAL

All synthetic reagents and solvents were obtained from reputable commercial suppliers such as Merck, Sigma-Aldrich, TCI, Spectrochem and Avra Chemicals. These chemicals were used directly without any additional purification. The progress of the reactions was monitored by thin-layer chromatography (TLC) on Merck silica gel $60F_{254}$ plates. Melting points of the final compounds were determined using a Stuart SMP3 apparatus and the values are reported without correction. Purification of the crude mixtures was carried out through recrystallisation and by column chromatography using ethyl acetate and *n*-hexane in a 10:90 ratio as the eluent system. The composition and functional groups of the synthesised compounds were confirmed by infrared spectroscopy using a Shimadzu FTIR 8400 S instrument with KBr pellets. ^{1}H and ^{13}C NMR spectra were recorded on a Bruker 400 MHz spectrometer operating at 400 MHz and 100 MHz, respectively, with $CDCl_3$ and DMSO-d_6 as solvents and TMS as the internal reference. Mass spectral data were obtained using a Shimadzu GC-MS QP 1000 system.

Synthesis of imidazole derivative (3): A mixture of 6-nitrobenzo[*d*][1,3]dioxole-5-carbaldehyde (**1**) (1.0 equiv.), benzil (**2**) (1.0 equiv.) and ammonium acetate (3.0-5.0 equiv.) was dissolved in glacial acetic acid (10-15 mL/mmol) in a round-bottom flask fitted with a reflux condenser. The reaction mixture was refluxed under continuous stirring for approximately 9 h and the progress of the reaction was monitored by TLC. After completion of the reaction, the mixture was allowed to cool to ambient temperature and then carefully poured into crushed ice-cold water (50-100 mL). The precipitated solid was filtered, washed thoroughly with cold water to remove residual acetic acid and inorganic impurities and dried under reduced pressure. Purification of the crude product by silica gel column chromatography using hexane/ethyl acetate as the eluent afforded the desired imidazole derivative (**3**) as a purified solid.

Synthesis of *N*-propargylated imidazole intermediate (4): Imidazole derivative (**3**) (1.0 equiv.) was dissolved in anhydrous DMF (10-15 mL/mmol) under a N_2 atmosphere followed by the addition of K_2CO_3 (2.0-2.5 equiv.) to the solution and the resulting mixture was stirred at room temperature for 15-20 min to facilitate deprotonation. Subsequently, propargyl bromide (1.2-1.5 equiv.) was added dropwise and the reaction mixture was heated under reflux for 6-12 h with continuous stirring. The reaction progress was periodically monitored by TLC. Upon completion, the reaction mixture was cooled to room temperature and poured into ice-cold water (~50 mL). The aqueous layer was extracted with ethyl acetate (3 × 25 mL) and the combined organic extracts were washed successively with water and brine solution. The organic phase was dried over anhydrous Na_2SO_4, filtered and concentrated under reduced pressure. The resulting crude residue was purified by silica gel column chromatography to obtain the corresponding *N*-propargylated imidazole intermediate (**4**).

General procedure for the synthesis of 1,2,3-triazole derivatives (6a-l): A solution of *N*-propargylated imidazole intermediate (**4**) (1.0 equiv.) and the corresponding aryl azide (1.1–1.3 equiv.) was prepared in DMF (8112 mL/mmol). To this solution, $CuSO_4 \cdot 5H_2O$ (0.1 equiv.) and sodium ascorbate (0.2 equiv.) were added sequentially under stirring. The reaction mixture was stirred at room temperature or heated at 40-60 ºC, depending on substrate reactivity, for 6-24 h. The progress of the cycloaddition reaction was monitored by TLC analysis. After completion, the reaction mixture was diluted with water (~ 50 mL) and extracted with ethyl acetate (3 × 25 mL). The combined organic layers were washed with brine solution, dried over anhydrous Na_2SO_4, filtered and concentrated under reduced pressure (**Scheme-I**). Purification of the crude product by silica gel column chromatography using hexane/ethyl acetate (4:6) or dichloromethane/methanol as the mobile phase afforded the desired 1,4-disubstituted 1,2,3-triazole derivatives (**6a-l**) in good yields.

2-(6-Nitrobenzo[*d*][1,3]dioxol-5-yl)-4,5-diphenyl-1-(prop-2-yn-1-yl)-1*H*-imidazole (4): Light yellow solid; yield: 78%; R_f: 0.62 (hexane/ethyl acetate, 6:4); m.p.: 196-198 ºC. IR (KBr, ν_{max}, cm^{-1}): 3290 (≡C-H *str*. of terminal alkyne), 3169 (N–H *str*.), 3090 (arom. =C-H *str*.), 1715 (C=N *str*. of imidazole ring), 1554 (arom. C=C *str*.), 1264 (C-O-C *str*. of benzodioxole moiety); ^{1}H NMR (400 MHz, $CDCl_3$, δ ppm): 7.68 (s, 1H, Ar-H), 7.54 (s, 1H, imidazole-H), 7.52 (s, 1H, Ar-H), 7.49 (d, *J* = 1.7 Hz, 2H, Ar-H), 7.48-7.47 (m, 2H, Ar-H), 7.20 (d, *J* = 7.1 Hz, 1H, Ar-H), 7.18 (s, 1H, Ar-H), 7.15 (d, *J* = 7.2 Hz, 1H, Ar-H), 6.21 (s, 2H, O-CH_2-O), 4.35 (s, 2H, N-CH_2), 2.28 (s, 1H, ≡C-H); ^{13}C NMR (100 MHz, $CDCl_3$, δ ppm): 149.19, 146.81, 141.38, 140.27, 135.50, 131.65, 128.67, 127.66, 126.86, 126.69, 126.58, 125.67, 124.43, 124.14, 119.72, 109.75, 103.31, 101.09, 75.66 (alkynyl carbon), 71.06 (alkynyl carbon), 32.00 (N-CH_2); ESI-MS: *m/z* 424.13 $[M + H]^+$.

1-(4-Bromophenyl)-4-((2-(6-nitrobenzo[*d*][1,3]dioxol-5-yl)-4,5-diphenyl-1*H*-imidazol-1-yl)methyl)-1*H*-1,2,3-triazole (6a): White solid; yield: 74%; R_f: 0.61 (hexane/ethyl acetate, 6:4); m.p.: 190-192 ºC. IR (KBr, ν_{max}, cm^{-1}): 3109 (arom. C-H *str*.), 1615 (C=N *str*. of imidazole/triazole ring), 1554 (arom. C=C *str*.), 1264 (C-O-C *str*. of benzodioxole moiety); ^{1}H NMR (400 MHz, $CDCl_3$, δ ppm): 7.64 (s, 2H, triazole-H), 7.60 (s, 1H, Ar-H), 7.46 (d, *J* = 2.2 Hz, 5H, Ar-H), 7.47-7.38 (m, 5H, Ar-H), 7.18 (d, *J* = 7.4 Hz, 2H, Ar-H), 7.15 (d, *J* = 3.7 Hz, 2H, Ar-H), 6.18 (s, 2H, O-CH_2-O), 5.10 (s, 2H, N-CH_2); ^{13}C NMR (100 MHz, $CDCl_3$, δ ppm): 163.12, 161.14, 151.45, 148.94, 143.25, 142.91, 137.91, 133.40, 132.55, 130.72, 130.32, 128.86, 128.70, 127.79, 126.53, 126.36, 122.09, 122.03, 121.68, 120.25, 116.50, 116.32, 111.81, 105.43, 103.23, 40.14 (N-CH_2); ESI-MS: *m/z* 561.16 $[M + H]^+$; Anal. calcd. (found) % for $C_{29}H_{20}BrN_6O_4$: C, 59.91 (59.82); H, 3.41 (3.44); N, 13.52 (13.53).

1-(4-Fluorophenyl)-4-((2-(6-nitrobenzo[*d*][1,3]dioxol-5-yl)-4,5-diphenyl-1*H*-imidazol-1-yl)methyl)-1*H*-1,2,3-triazole (6b): Yellow solid; yield: 76%; R_f: 0.58 (hexane/ethyl acetate, 6:4); m.p.: 186-188 ºC. IR (KBr, ν_{max}, cm^{-1}): 3104

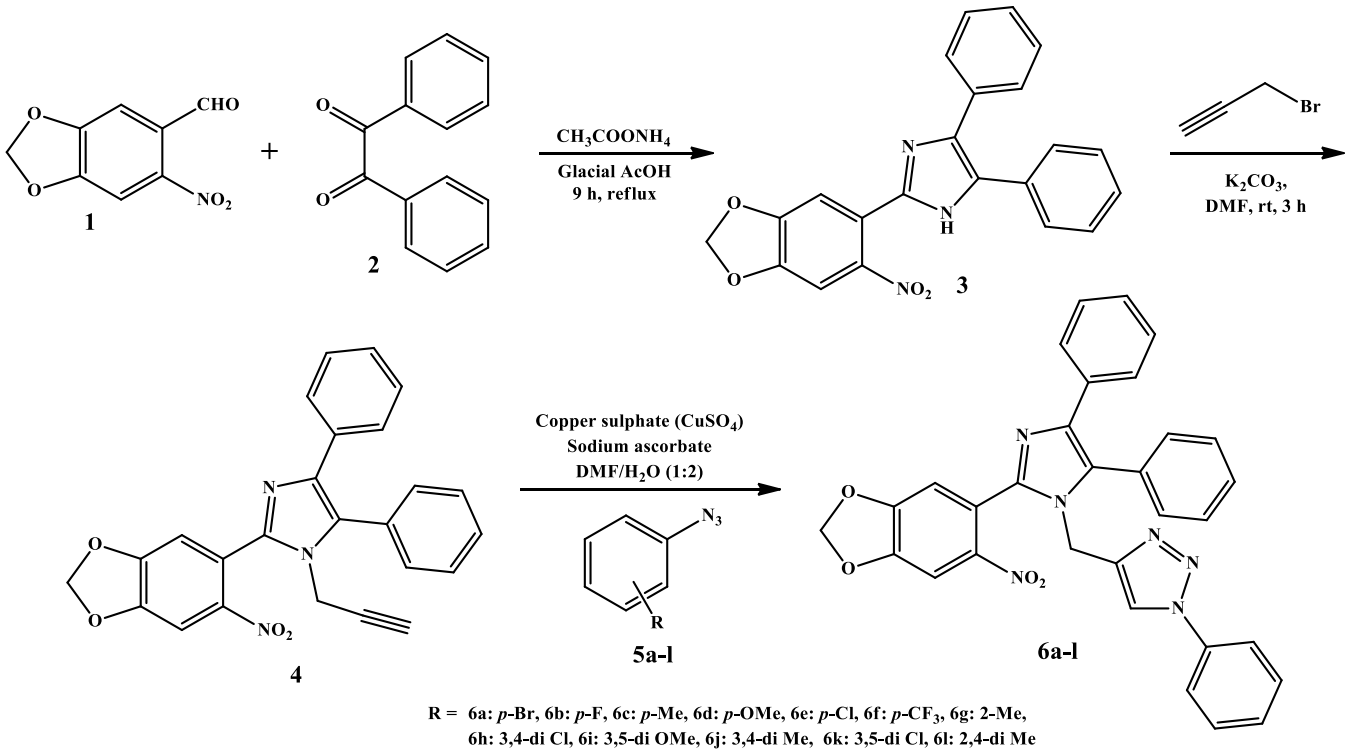

Scheme-I: General synthetic pathway for the preparation of targeted imidazole–triazole derivatives (**6a-l**)

(arom. C-H *str.*), 1619 (C=N *str.* of heterocyclic ring), 1557 (arom. C=C *str.*), 1260 (C-O-C *str.*); ^{1}H NMR (400 MHz, $CDCl_3$, δ ppm): 7.69 (d, *J* = 2.1 Hz, 1H, Ar-H), 7.65 (s, 1H, triazole-H), 7.56 (d, *J* = 8.7 Hz, 2H, Ar-H), 7.46 (d, *J* = 3.5 Hz, 6H, Ar-H), 7.39 (d, *J* = 6.0 Hz, 3H, Ar-H), 7.18 (d, *J* = 5.0 Hz, 2H, Ar-H), 7.14 (d, *J* = 13.6 Hz, 2H, Ar-H), 6.19 (s, 2H, O-CH_2-O), 5.10 (s, 2H, N-CH_2); ^{13}C NMR (100 MHz, $CDCl_3$, δ ppm): 163.51, 161.53, 151.84, 149.33, 143.64, 143.30, 138.30, 133.79, 132.94, 131.11, 129.25, 129.09, 128.18, 126.92, 126.75, 122.48, 122.07, 120.64, 116.89, 116.71, 112.20, 105.82, 103.62, 40.53 (N-CH_2); ESI-MS: *m/z* 557.21 $[M + H]^+$; Anal. calcd. (found) % for $C_{29}H_{20}FN_6O_4$: C, 66.42 (66.47); H, 3.78 (3.70); N, 14.99 (14.82).

4-((2-(6-Nitrobenzo[*d*][1,3]dioxol-5-yl)-4,5-diphenyl-1*H*-imidazol-1-yl)methyl)-1-(*p*-tolyl)-1*H*-1,2,3-triazole (6c): Golden yellow solid; yield: 79%; R_f: 0.64 (hexane/ethyl acetate, 6:4); m.p.: 194-198 ºC. IR (KBr, ν_{max}, cm^{-1}): 3100 (arom. C-H *str.*), 1610 (C=N *str.*), 1564 (arom. C=C *str.*), 1254 (C-O-C *str.* of benzodioxole ring); ^{1}H NMR (400 MHz, $CDCl_3$, δ ppm): 7.95 (s, 1H, triazole-H), 7.57 (s, 2H, Ar-H), 7.36 (d, *J* = 9.6 Hz, 6H, Ar-H), 7.18 (s, 2H, Ar-H), 7.08 (d, *J* = 8.9 Hz, 3H, Ar-H), 6.97 (s, 2H, Ar-H), 6.07 (s, 2H, O-CH_2-O), 5.01 (s, 2H, N-CH_2), 2.87 (s, 3H, CH_3); ^{13}C NMR (101 MHz, $CDCl_3$, δ ppm): 151.82, 149.35, 143.63, 142.65, 138.27, 136.09, 133.58, 131.50, 131.08, 130.63, 130.04, 129.22, 129.08, 128.17, 126.96, 126.86, 126.72, 125.81, 123.62, 112.36, 105.79, 103.60, 40.54 (N-CH_2), 17.79 (CH_3); ESI-MS: *m/z* 557.19 $[M + H]^+$; Anal. calcd. (found) % for $C_{30}H_{23}N_6O_4$: C, 69.06 (69.16); H, 4.35 (4.39); N, 15.10 (15.17).

1-(4-Methoxyphenyl)-4-((2-(6-nitrobenzo[*d*][1,3]dioxol-5-yl)-4,5-diphenyl-1*H*-imidazol-1-yl)methyl)-1*H*-1,2,3-triazole (6d): White solid; yield: 81%; R_f: 0.63 (hexane/ethyl acetate, 6:4); m.p.: 185-187 ºC. IR (KBr, ν_{max}, cm^{-1}): 3119 (arom. C-H *str.*), 1625 (C=N *str.* of heterocyclic ring), 1553 (arom. C=C *str.*), 1264 (C-O-C *str.* of benzodioxole/methoxy group); ^{1}H NMR (400 MHz, $CDCl_3$, δ ppm): 7.60 (s, 1H, triazole-H), 7.44 (d, *J* = 7.3 Hz, 3H, Ar-H), 7.41 (dd, *J* = 8.5, 5.8 Hz, 5H, Ar-H), 7.16 (d, *J* = 6.0 Hz, 2H, Ar-H), 7.09 (s, 3H, Ar-H), 6.70 (s, 2H, Ar-H), 6.13 (s, 2H, O-CH_2-O), 5.06 (s, 2H, N-CH_2), 3.86 (s, 3H, OCH_3); ^{13}C NMR (101 MHz, $CDCl_3$, δ ppm): 154.13, 151.65, 145.94, 144.93, 138.39, 135.89, 133.80, 133.39, 132.94, 132.34, 131.53, 131.39, 130.47, 129.26, 129.17, 129.03, 128.12, 125.92, 114.67, 108.10, 105.90, 55.84 (OCH_3), 42.84 (N-CH_2); ESI-MS: *m/z* 573.41 $[M + H]^+$. Anal. calcd. (found) % for $C_{30}H_{23}N_6O_5$: C, 67.13 (67.17); H, 4.22 (4.20); N, 14.68 (14.61).

1-(4-Chlorophenyl)-4-((2-(6-nitrobenzo[*d*][1,3]dioxol-5-yl)-4,5-diphenyl-1*H*-imidazol-1-yl)methyl)-1*H*-1,2,3-triazole (6e): Light yellow solid; yield: 77%; R_f: 0.60 (hexane/ethyl acetate, 6:4); m.p.: 194-196 ºC. IR (KBr, ν_{max}, cm^{-1}): 3101 (arom. C-H *str.*), 1613 (C=N *str.*), 1558 (arom. C=C *str.*), 1262 (C-O-C *str.*); ^{1}H NMR (400 MHz, $CDCl_3$, δ ppm): 7.63 (d, *J* = 4.7 Hz, 2H, Ar-H), 7.60 (s, 2H, triazole-H), 7.44 (s, 3H, Ar-H), 7.41 (s, 4H, Ar-H), 7.19 (s, 2H, Ar-H), 7.14 (d, *J* = 4.3 Hz, 3H, Ar-H), 6.17 (s, 2H, O-CH_2-O), 5.10 (s, 2H, N-CH_2); ^{13}C NMR (100 MHz, $CDCl_3$, δ ppm): 166.11, 164.12, 154.43, 151.93, 146.24, 145.90, 140.90, 136.39, 135.54, 133.71, 133.31, 131.85, 131.69, 130.78, 129.52, 129.35, 125.08, 125.02, 124.67, 123.24, 119.49, 119.31, 114.80, 108.42, 106.21, 43.12 (N-CH_2); ESI-MS: *m/z* 577.43 $[M + H]^+$. Anal. calcd. (found) % for $C_{29}H_{20}ClN_6O_4$: C, 64.53 (64.56); H, 3.67 (3.61); N, 14.57 (14.52).

4-((2-(6-Nitrobenzo[*d*][1,3]dioxol-5-yl)-4,5-diphenyl-1*H*-imidazol-1-yl)methyl)-1-(4-(trifluoromethyl)phenyl)-1*H*-1,2,3-triazole (6f): Yellow solid; yield: 73%; R_f: 0.57

(hexane/ethyl acetate, 6:4); m.p.: 187-189 ºC. IR (KBr, ν_{max}, cm^{-1}): 3102 (arom. C-H *str.*), 1619 (C=N *str.* of heterocyclic ring), 1550 (arom. C=C *str.*), 1264 (C-O-C *str.*); ^{1}H NMR (400 MHz, $CDCl_3$, δ ppm): 7.79 (s, 1H, triazole-H), 7.75 (d, *J* = 7.6 Hz, 1H, Ar-H), 7.69 (d, *J* = 7.6 Hz, 1H, Ar-H), 7.66-7.62 (m, 2H, Ar-H), 7.48 (s, 4H, Ar-H), 7.42 (s, 2H, Ar-H), 7.21-7.17 (m, 2H, Ar-H), 7.14 (d, *J* = 3.4 Hz, 3H, Ar-H), 6.18 (s, 2H, O-CH_2-O), 5.12 (s, 2H, N-CH_2); ^{13}C NMR (100 MHz, $CDCl_3$, δ ppm): 151.64, 149.26, 143.83, 142.72, 137.95, 134.10, 134.03, 131.12, 130.11, 129.31, 129.14, 129.03, 128.12, 126.87, 126.59, 122.17, 112.20, 105.76, 103.54, 124.15 (CF_3-substituted carbon), 43.45 (N-CH_2); ESI-MS: *m/z* 611.16 $[M + H]^+$; Anal. calcd. (found) % for $C_{30}H_{20}F_3N_6O_4$: C, 62.95 (62.91); H, 3.47 (3.42); N, 13.76 (13.70).

4-((2-(6-Nitrobenzo[*d*][1,3]dioxol-5-yl)-4,5-diphenyl-1*H*-imidazol-1-yl)methyl)-1-(o-tolyl)-1*H*-1,2,3-triazole (6g): White solid; yield: 80%; R_f: 0.65 (hexane/ethyl acetate, 6:4); m.p.: 187-189 ºC. IR (KBr, ν_{max}, cm^{-1}): 3112 (arom. C-H *str.*), 1610 (C=N *str.*), 1555 (arom. C=C *str.*), 1263 (C-O-C *str.*); ^{1}H NMR (400 MHz, $CDCl_3$, δ ppm): 8.08 (d, *J* = 5.7 Hz, 2H, Ar-H), 7.65 (s, 1H, triazole-H), 7.43 (d, *J* = 8.1 Hz, 6H, Ar-H), 7.19 (dd, *J* = 1.4, 8.1 Hz, 4H, Ar-H), 6.18 (s, 2H, O-CH_2-O), 5.12 (s, 2H, N-CH_2), 2.64 (s, 3H, CH_3). ^{13}C NMR (101 MHz, $CDCl_3$, δ ppm): 163.57, 152.84, 150.36, 144.28, 140.77, 139.94, 137.60, 137.52, 132.16, 131.56, 131.44, 130.22, 130.10, 129.19, 127.79, 121.35, 119.19, 113.15, 106.75, 104.63, 37.51 (N-CH_2), 22.28 (CH_3). ESI-MS *m/z*: 557.20 $[M + H]^+$; Anal. calcd. (found) % for $C_{30}H_{23}N_6O_4$: C, 69.06 (69.09); H, 4.35 (4.38); N, 15.10 (15.12).

1-(3,4-Dichlorophenyl)-4-((2-(6-nitrobenzo[*d*][1,3]dioxol-5-yl)-4,5-diphenyl-1*H*-imidazol-1-yl)methyl)-1*H*-1,2,3-triazole (6h): Light yellow solid; yield: 75%; R_f: 0.59 (hexane/ethyl acetate, 6:4); m.p.: 192-194 ºC. IR (KBr, ν_{max}, cm^{-1}): 3109 (arom. C-H *str.*), 1611 (C=N *str.* of heterocyclic ring), 1550 (arom. C=C *str.*), 1254 (C-O-C *str.* of benzodioxole moiety). ^{1}H NMR (400 MHz, $CDCl_3$, δ ppm): 7.71-7.64 (m, 1H, Ar-H), 7.61 (s, 1H, triazole-H), 7.56 (d, *J* = 8.7 Hz, 1H, Ar-H), 7.46 (d, *J* = 3.5 Hz, 4H, Ar-H), 7.39 (d, *J* = 6.0 Hz, 3H, Ar-H), 7.21-7.15 (m, 2H, Ar-H), 7.12 (s, 3H, Ar-H), 6.19 (s, 2H, O-CH_2-O), 5.10 (s, 2H, N-CH_2); ^{13}C NMR (100 MHz, $CDCl_3$, δ ppm): 151.84, 149.32, 143.97, 135.63, 134.07, 133.19, 131.54, 131.12, 129.31, 129.11, 128.19, 126.87, 126.75, 122.23, 122.08, 120.35, 119.31, 105.85, 103.62, 40.49 (N-CH_2); ESI-MS *m/z*: 612.09 $[M + H]^+$; Anal. calcd. (found) % for $C_{29}H_{19}Cl_2N_6O_4$: C, 60.89 (60.81); H, 3.30 (3.32); N, 13.74 (13.71).

1-(3,5-Dimethoxyphenyl)-4-((2-(6-nitrobenzo[*d*][1,3]-dioxol-5-yl)-4,5-diphenyl-1*H*-imidazol-1-yl)methyl)-1*H*-1,2,3-triazole (6i): Yellow solid; yield: 78%; R_f: 0.62 (hexane/ethyl acetate, 6:4); m.p.: 185-187 ºC. IR (KBr, ν_{max}, cm^{-1}): 3119 (arom. C-H *str.*), 1610 (C=N *str.*), 1549 (arom. C=C *str.*), 1254 (C-O-C *str.*); ^{1}H NMR (400 MHz, $CDCl_3$, δ ppm): 7.65 (s, 1H, triazole-H), 7.49 (d, *J* = 7.3 Hz, 3H, Ar-H), 7.46-7.40 (m, 5H, Ar-H), 7.21 (d, *J* = 6.0 Hz, 2H, Ar-H), 7.15 (d, *J* = 10.1 Hz, 3H, Ar-H), 6.75 (s, 2H, Ar-H), 6.18 (s, 2H, O-CH_2-O), 5.10 (s, 2H, N-CH_2), 3.88 (s, 6H, 2 × OCH_3). ^{13}C NMR (100 MHz, $CDCl_3$, δ ppm): 148.93, 146.84, 144.30, 138.64, 138.45, 138.22, 133.44, 133.31, 128.94, 128.80, 127.47, 126.16, 125.80, 124.26, 124.00, 123.19, 121.90, 121.76, 117.10, 115.70, 107.16, 100.85, 98.61, 93.30, 56.08 (OCH_3), 51.47 (OCH_3), 35.54 (N-CH_2); ESI-MS: *m/z* 603.19 $[M + H]^+$; Anal. calcd. (found) % for $C_{31}H_{25}N_6O_6$: C, 65.77 (65.71); H, 4.35 (4.37); N, 13.95 (13.93).

1-(3,4-Dimethylphenyl)-4-((2-(6-nitrobenzo[*d*][1,3]-dioxol-5-yl)-4,5-diphenyl-1*H*-imidazol-1-yl)methyl)-1*H*-1,2,3-triazole (6j): White solid; yield: 80%; R_f: 0.64 (hexane/ethyl acetate, 6:4); m.p.: 190-192 ºC. IR (KBr, ν_{max}, cm^{-1}): 3104 (arom. C-H *str.*), 1612 (C=N *str.*), 1551 (arom. C=C *str.*), 1260 (C-O-C *str.*); ^{1}H NMR (400 MHz, $CDCl_3$, δ ppm): 7.65 (s, 1H, triazole-H), 7.53 (d, *J* = 8.2 Hz, 3H, Ar-H), 7.43 (d, *J* = 8.0 Hz, 3H, Ar-H), 7.32 (s, 1H, Ar-H), 7.26 (s, 2H, Ar-H), 7.21 (s, 4H, Ar-H), 7.11 (s, 2H, Ar-H), 6.15 (s, 2H, O-CH_2-O), 5.07 (s, 2H, N-CH_2), 2.31 (s, 6H, 2 × CH_3); ^{13}C NMR (101 MHz, $CDCl_3$, δ ppm): 151.79, 149.28, 143.61, 143.28, 138.43, 137.80, 134.58, 133.89, 131.17, 130.65, 129.23, 129.04, 128.15, 126.91, 126.67, 122.24, 121.57, 120.54, 120.39, 117.67, 112.32, 105.74, 103.56, 40.56 (N-CH_2), 19.94, 19.49 (2 × CH_3); ESI-MS *m/z*: 571.20 $[M + H]^+$; Anal. calcd. (found) % for $C_{32}H_{27}N_6O_4$: C, 69.46 (69.41); H, 4.59 (4.52); N, 14.73 (14.77).

1-(3,5-Dichlorophenyl)-4-((2-(6-nitrobenzo[*d*][1,3]-dioxol-5-yl)-4,5-diphenyl-1*H*-imidazol-1-yl)methyl)-1*H*-1,2,3-triazole (6k): White solid; yield: 74%; R_f: 0.58 (hexane/ethyl acetate, 6:4); m.p.: 192-194 ºC. IR (KBr, ν_{max}, cm^{-1}): 3104 (arom. C-H *str.*), 1612 (C=N *str.*), 1551 (arom. C=C *str.*), 1271 (C-O-C *str.*); ^{1}H NMR (400 MHz, $CDCl_3$, δ ppm): 7.58 (s, 1H, triazole-H), 7.40 (s, 3H, Ar-H), 7.40 (s, 2H, Ar-H), 7.34 (s, 3H, Ar-H), 7.11 (d, *J* = 6.7 Hz, 3H, Ar-H), 7.04 (d, *J* = 8.8 Hz, 3H, Ar-H), 6.12 (s, 2H, O-CH_2-O), 5.02 (s, 2H, N-CH_2); ^{13}C NMR (100 MHz, $CDCl_3$, δ ppm): 141.84, 139.32, 133.97, 133.88, 133.70, 129.61, 125.63, 124.07, 123.19, 121.54, 121.12, 119.31, 119.11, 118.19, 116.86, 116.75, 112.23, 112.08, 110.35, 109.31, 102.16, 95.85, 93.62, 30.49 (N-CH_2); ESI-MS: *m/z* 612.09 $[M + H]^+$; Anal. calcd. (found) % for $C_{29}H_{19}Cl_2N_6O_4$: C, 60.89 (60.82); H, 3.30 (3.32); N, 13.74 (13.78).

1-(2,4-Dimethylphenyl)-4-((2-(6-nitrobenzo[*d*][1,3]-dioxol-5-yl)-4,5-diphenyl-1*H*-imidazol-1-yl)methyl)-1*H*-1,2,3-triazole (6l): Light yellow solid; yield: 79%; R_f: 0.63 (hexane/ethyl acetate, 6:4); m.p.: 190-192 ºC. IR (KBr, ν_{max}, cm^{-1}): 3109 (arom. C-H *str.*), 1612 (C=N *str.* of heterocyclic ring), 1554 (arom. C=C *str.*), 1260 (C-O-C *str.*); ^{1}H NMR (400 MHz, $CDCl_3$, δ ppm): 7.66 (s, 1H, triazole-H), 7.48 (d, *J* = 9.6 Hz, 2H, Ar-H), 7.43 (dd, *J* = 9.6, 2.9 Hz, 3H, Ar-H), 7.18 (d, *J* = 7.5 Hz, 2H, Ar-H), 7.13 (d, *J* = 5.9 Hz, 3H, Ar-H), 6.17 (s, 2H, O-CH_2-O), 5.09 (s, 2H, N-CH_2), 2.40 (s, 3H, CH_3), 2.04 (s, 3H, CH_3); ^{13}C NMR (100 MHz, $CDCl_3$, δ ppm): 153.93, 151.84, 149.30, 143.64, 143.45, 143.22, 138.44, 133.80, 132.47, 131.16, 130.80, 129.26, 129.00, 128.19, 126.90, 126.76, 122.10, 120.70, 112.16, 105.85, 103.61, 40.54 (N-CH_2), 21.30 and 19.47 (2 × CH_3); ESI-MS *m/z*: 571.20 $[M + H]^+$; Anal. calcd. (found) % for $C_{32}H_{27}N_6O_4$: C, 69.46 (69.41); H, 4.59 (4.51); N, 14.73 (14.77).

Cytotoxicity studies: The synthesised compounds **6a-l** were evaluated for their *in vitro* anticancer activity using the MTT assay, a standard colorimetric method based on mitochondrial metabolic activity. Human breast cancer cells (MCF-7) were employed to determine anticancer potential, while mouse fibroblast cells (NIH/3T3) were used to assess cytotoxic selec-

tivity toward normal cells. The compounds were tested at concentrations ranging from 12-400 μM to generate dose–response curves and determine IC_{50} values. Doxorubicin was used as the reference anticancer drug for comparative evaluation. All experiments were performed in triplicate and results are expressed as mean ± SD. Statistical analysis was carried out using one-way ANOVA at a significance level of $p < 0.05$.

Antibacterial activity: The synthesised compounds **6a-l**, bearing different substituents at the R-position, were systematically evaluated for their antibacterial activity against selected Gram-positive bacteria, *Staphylococcus aureus* and *Bacillus subtilis* and Gram-negative bacteria, *Klebsiella pneumoniae* and *Escherichia coli*. The antibacterial screening was carried out at concentrations of 10 μg/mL and 20 μg/mL using the agar disc diffusion method, with gatifloxacin employed as the reference standard.

Antifungal activity: The synthesised compounds **6a-l**, containing different substituents, were evaluated for their *in vitro* antifungal activity against *Aspergillus niger*, *Aspergillus flavus* and *Fusarium oxysporum* at a 50 μg/mL using the agar disc diffusion method. The antifungal efficacy was expressed as the zone of inhibition (mm) and compared with the standard antifungal drug clotrimazole.

Molecular docking: Molecular docking studies were performed to predict the binding interactions of the synthesised compounds with the epidermal growth factor receptor (EGFR), a key therapeutic target associated with cancer progression. The crystal structure of EGFR (PDB ID: 2J6M) was retrieved from the Protein Data Bank and docking simulations were carried out using AutoDock Vina integrated within the PyRx virtual screening platform. Ligand structures were drawn using ChemDraw Professional 16.0, energy-minimized and converted to PDBQT format. Protein preparation involved removal of water molecules and heteroatoms, followed by the addition of polar hydrogen atoms. Docking calculations were conducted using a defined active-site grid box with an exhaustiveness value of 8. The resulting protein–ligand interactions and binding conformations were analysed using PyMOL and BIOVIA Discovery Studio.

RESULTS AND DISCUSSION

A series of novel imidazole–triazole hybrid derivatives was synthesized through a multistep synthetic strategy, as outlined in **Scheme-I**. Initially, 6-nitrobenzo[*d*][1,3]dioxole-5-carbaldehyde (**1**) was reacted with benzil (**2**) in the presence of ammonium acetate and glacial acetic acid under reflux conditions to afford the corresponding imidazole derivative (**3**) *via* a Debus-Radziszewski type cyclocondensation reaction. The synthesized imidazole derivative was subsequently subjected to *N*-alkylation with propargyl bromide in dry DMF using K_2CO_3 as base, yielding the corresponding *N*-propargylated intermediate (**4**). The introduction of the propargyl moiety provided a terminal alkyne functionality suitable for further click chemistry transformations. The propargylated intermediate was then reacted with various aryl azides under Cu(I) catalysed azide–alkyne cycloaddition (CuAAC) conditions using $CuSO_4$ and sodium ascorbate in DMF to furnish the desired 1,2,3-triazole derivatives (**6a-l**). The CuAAC reaction proceeded through *in situ* generation of Cu(I), followed by formation of a copper acetylide intermediate and regioselective cycloaddition with the azide to obtain the 1,4-disubstituted triazole ring system.

Reaction conditions for the cycloaddition process were optimized using different solvents and the results are summarized in Table-1. Solvent polarity and solubility significantly affected reaction efficiency and product yield. Among the investigated systems, DMF/H_2O mixtures exhibited superior performance, with DMF/H_2O (1:2) providing the highest yield (88%) under room-temperature conditions. The enhanced efficiency was attributed to improved catalyst solubility, effective *in situ* Cu(I) generation, and favourable aqueous organic synergistic effects that promoted the click reaction.

TABLE-1
OPTIMISATION OF SOLVENT CONDITIONS FOR THE CLICK REACTION

Entry	Solvent	Temp. (ºC)	Time (h)	Yield (%)
1	Methanol	65	12	58
2	Ethanol	78	10	65
3	Acetonitrile	82	9	61
4	DMF	RT	8	68
5	Toluene	110	11	52
6	DMF/H_2O (1:2)	RT	9	88
7	DMF/H_2O (1:3)	RT	8	82
8	Water (H_2O)	RT	14	45

Cytotoxicity: The cytotoxicity results (Table-2) demonstrate that the synthesised imidazole–triazole derivatives (**6a-l**) exhibited varying degrees of anticancer activity against the MCF-7 breast cancer cell line. The obtained IC_{50} values indicate that the nature as well as the position of substituents attached to the aryl ring significantly influence biological activity. Among all evaluated compounds, derivative **6f** bearing a *para*-trifluoromethyl (-CF_3) substituent displayed the highest anticancer potency with an IC_{50} value of 0.69 ± 1.95 μM, surpassing the activity of the standard drug doxorubicin (IC_{50} = 2.92 ± 1.26 μM). The enhanced activity of this compound may be attributed to the strong electron-withdrawing and lipophilic characteristics of the -CF_3 group, which can improve molecular interactions with the biological target and facilitate better cellular penetration.

TABLE-2
IC_{50} VALUES (μM) FOR SYNTHESISED COMPOUNDS **6a-l**

Compound	IC_{50} ± SD (μM)	
	MCF-7	NIH/3T3
6a	2.41 ± 0.16	10.84 ± 1.19
6b	2.70 ± 1.47	9.71 ± 0.22
6c	2.41 ± 0.92	10.19 ± 0.48
6d	1.10 ± 0.28	6.98 ± 0.13
6e	1.06 ± 0.50	9.84 ± 0.36
6f	0.69 ± 1.95	7.52 ± 0.72
6g	4.77 ± 1.47	14.71 ± 0.72
6h	1.82 ± 0.18	8.19 ± 0.85
6i	1.06 ± 0.50	9.84 ± 0.36
6j	2.11 ± 1.92	12.09 ± 0.58
6k	1.79 ± 0.45	8.50 ± 0.55
6l	2.55 ± 0.96	8.55 ± 0.88
Doxorubicin	2.92 ± 1.26	11.81 ± 1.34

Compounds **6d** and **6e** also exhibited remarkable cytotoxic activity with IC_{50} values of 1.10 ± 0.28 and 1.06 ± 0.50 μM, respectively. The high potency observed for the methoxy substituted derivative (**6d**) suggests that electron-donating substituents are capable of enhancing biological activity, possibly through improved electronic distribution and favourable intermolecular interactions. Similarly, *para*-chloro substituted derivative (**6e**) demonstrated excellent activity, indicating that halogen substituents also contribute positively toward anticancer potential. Compound **6i** containing two methoxy substituents (3,5-dimethoxy) showed comparable activity (IC_{50} = 1.06 ± 0.50 μM), further supporting the beneficial influence of methoxy groups on cytotoxic activity.

The dichloro-substituted compounds **6h** and **6k** demonstrated good anticancer activity with IC_{50} values of 1.82 ± 0.18 and 1.79 ± 0.45 μM, respectively. These results indicate that the presence of multiple halogen substituents can favourably modulate biological activity through electronic and hydrophobic effects. In contrast, compounds **6a**, **6b**, **6c**, **6j** and **6l** exhibited only moderate cytotoxic activity with IC_{50} values ranging from 2.11 to 2.70 μM. Although these derivatives retained appreciable activity, their potency was lower than that observed for strongly electron-withdrawing or methoxy-substituted analogues.

Among all the synthesised compounds, derivative **6g** containing an *ortho*-methyl substituent displayed the lowest anticancer activity with an IC_{50} value of 4.77 ± 1.47 μM. The reduced activity of this compound may be attributed to steric hindrance caused by substitution at the *ortho* position, which can disturb molecular planarity and reduce effective interaction with the biological target site. This observation highlights the importance of substituent orientation in determining biological response.

Evaluation of the synthesized compounds against the NIH/3T3 normal fibroblast cell line revealed comparatively lower toxicity toward normal cells, with IC_{50} values ranging from 6.98 ± 0.13 to 14.71 ± 0.72 μM. The observed difference in cytotoxicity between cancerous and normal cell lines indicates selective activity toward malignant cells, highlighting the potential therapeutic significance of the synthesized imidazole–triazole hybrids. The results presented in Table-2 demonstrate that both electronic and steric factors significantly influence the anticancer activity of the synthesized derivatives. In particular, the presence of strong electron-withdrawing groups such as -CF_3, along with suitable electron donating substituents such as methoxy groups, contributed to enhanced cytotoxic potency. Among the investigated compounds, derivative **6f** exhibited the most promising anticancer activity and emerged as a potential lead candidate for further biological and mechanistic studies.

Antibacterial activity: The antibacterial activity of the synthesised compounds **6a-l**, bearing different substituents at the aromatic ring, was evaluated against Gram-positive (*S. aureus* and *B. subtilis*) and Gram-negative (*E. coli* and *K. pneumoniae*) bacteria at concentrations of 10 and 20 μg/mL using the agar disc diffusion method. Gatifloxacin was used as the standard. Table-3 indicates that antibacterial activity was significantly influenced by the nature and position of the substituents. Among all synthesized derivatives, compound **6d** (*p*-OMe) exhibited the highest antibacterial activity, particularly against Gram-positive bacteria, with inhibition zones of 27.7 mm against *S. aureus* and 25.1 mm against *B. subtilis* at 20 μg/mL, exceeding the activity of the standard drug. Compounds **6e** (*p*-Cl) and **6f** (p-CF_3) also showed strong antibacterial potency, highlighting the favourable effect of electron-withdrawing substituents.

Halogenated derivatives such as **6a** (*p*-Br), **6b** (*p*-F), **6h** (3,4-diCl) and **6k** (3,5-diCl) demonstrated moderate to enhanced antibacterial activity, especially against Gram-positive strains. In contrast, derivatives containing electron-donating groups, including **6c** (*p*-Me), **6i** (3,5-diOMe), and **6j** (3,4-diMe), displayed only moderate activity, while **6g** (2-Me) showed comparatively lower potency, indicating the influence of substituent position on antibacterial behaviour. Based on

TABLE-3
ANTIMICROBIAL ACTIVITY OF SYNTHESISED COMPOUNDS **6a-l** AT DIFFERENT CONCENTRATIONS

Compound	Zone of inhibition (mm): Antibacterial activity								Zone of inhibition (mm) at 50 μg/mL concentration		
	Gram positive bacteria				Gram negative bacteria						
	S. aeureus		*B. subtilis*		*E. coli*		*K. pneumonia*		Antifungal activity		
	10 μg/mL	20 μg/mL	10 μg/mL	20 μg/mL	10 μg/mL	20 μg/mL	10 μg/mL	20 μg/mL	*A. niger*	*A. flavus*	*F. sporum*
6a	19.8	21.8	17.2	19.8	15.2	16.7	14.0	15.9	16.5	14.9	13.9
6b	20.1	22.6	18.9	20.4	15.9	16.2	14.8	16.4	15.8	17.9	18.7
6c	20.8	22.0	18.0	20.7	15.0	16.0	15.1	15.0	13.3	15.5	14.6
6d	24.9	27.7	21.8	25.1	18.2	19.0	16.9	19.7	25.4	24.8	25.0
6e	22.9	25.1	20.9	23.7	16.2	18.9	15.7	17.2	24.6	23.8	25.6
6f	21.2	23.7	22.2	22.8	16.2	19.9	16.8	19.0	25.9	26.2	24.8
6g	19.3	20.7	17.8	18.7	14.7	16.7	16.4	17.5	15.2	14.8	16.2
6h	21.2	23.7	21.2	23.4	16.2	19.1	17.9	18.9	23.4	22.5	24.5
6i	21.2	23.7	23.9	22.6	16.2	18.0	18.2	19.8	20.6	22.3	23.5
6j	19.1	20.9	18.4	19.4	15.1	16.2	16.8	15.9	17.6	16.8	18.6
6k	21.2	23.7	20.1	22.9	16.2	18.5	16.4	17.9	18.2	22.1	22.3
6l	19.2	20.9	21.3	22.6	15.4	18.7	14.4	15.6	14.9	19.8	19.8
Gatifloxacin	21.2	23.7	19.8	20.1	16.2	17.5	15.9	16.5	–	–	–
Clotrimazole	–	–	–	–	–	–	–	–	17.3	20.4	21.2

this, Gram-positive bacteria were more susceptible than Gram-negative strains. The SAR analysis suggests that *para*-substitution and halogen incorporation enhance antibacterial activity, with compound **6d** identified as the most promising antibacterial candidate.

Antifungal activity: The synthesised compounds **6a-l**, bearing different substituents on the aromatic ring, were evaluated for their *in vitro* antifungal activity against *Aspergillus niger*, *Aspergillus flavus* and *Fusarium oxysporum* at a concentration of 50 µg/mL using the poison plate method. The antifungal efficacy was expressed as the zone of inhibition (mm) and compared with standard clotrimazole.

The antifungal activity results (Table-3) demonstrate that the nature and position of substituents significantly influence biological activity. Among the synthesized derivatives, compound **6f** (*p*-CF_3) exhibited the highest antifungal activity against all tested fungal strains, showing inhibition zones greater than the standard drug. Compounds **6d** (*p*-OMe) and **6e** (*p*-Cl) also displayed strong broad-spectrum antifungal activity indicating the favorable contribution of both electron withdrawing and electron-donating substituents at the *para* position. Moreover, the di-halogenated derivative **6h** (3,4-diCl) showed enhanced antifungal potency, suggesting the beneficial effect of multiple electron-withdrawing groups. In contrast, derivatives containing electron-donating substituents such as **6i** (3,5-diOMe) and **6j** (3,4-diMe) exhibited moderate activity, while mono-substituted derivatives **6a** (*p*-Br), **6b** (*p*-F) and **6c** (*p*-Me) showed comparatively lower inhibition. Compound **6g** (2-Me) also displayed reduced activity, highlighting the influence of steric and positional effects on antifungal performance.

The SAR analysis revealed that *para*-substitution and the presence of halogen groups significantly enhance antifungal activity. Among the synthesized derivatives, compounds **6f**, **6d** and **6e** emerged as the most promising antimicrobial candidates. Significantly, compound **6f** exhibited superior antibacterial and antifungal activity compared with the standard drugs gatifloxacin and clotrimazole, highlighting its potential for further biological and anticancer investigations.

Molecular docking studies: The epidermal growth factor receptor (EGFR) is a transmembrane tyrosine kinase receptor that plays a crucial role in regulating cellular proliferation, differentiation, migration, and survival. Unusual activation or overexpression of EGFR has been closely associated with the progression of several cancers, making it an important target in anticancer drug discovery [22,23]. To evaluate the binding potential of the synthesized compounds toward EGFR, molecular docking studies were performed using the crystal structure of the EGFR tyrosine kinase domain (PDB ID: 6LUD). The docking protocol was validated by re-docking the co-crystallized ligand osimertinib, which produced an RMSD value of 1.12 Å, confirming the reliability of the docking methodology.

Based on cytotoxicity results, compounds **6f** and **6a** were selected for docking analysis. Among them, compound **6f** exhibited the highest binding affinity with a docking score of -9.4 kcal/mol, which was slightly better than the reference inhibitor osimertinib (-8.8 kcal/mol) (Table-4). The enhanced affinity of compound **6f** may be attributed to the presence of *p*-trifluoro-methyl substituent, which favours hydrophobic interactions within the binding pocket. Compound **6f** formed a key hydrogen bond with SER797 at a bond distance of 2.77 Å and also established hydrophobic interactions with residues Leu718, Ala743, Val726, His805 and Leu844, contributing to stable ligand accommodation within the EGFR active site (Fig. 2). Compound **6a** also showed favourable binding interactions but exhibited a comparatively lower docking score, correlating with its reduced cytotoxic activity. The reference ligand osimertinib formed hydrogen-bond interactions with Lys745 and Arg841 along with π-π stacking interactions involving Phe723 (Fig. 3). Thus, the docking analysis indicated that the synthesised compounds occupy the ATP-binding region of EGFR in a manner comparable to osimertinib, supporting their potential as promising EGFR-targeted anticancer candidates.

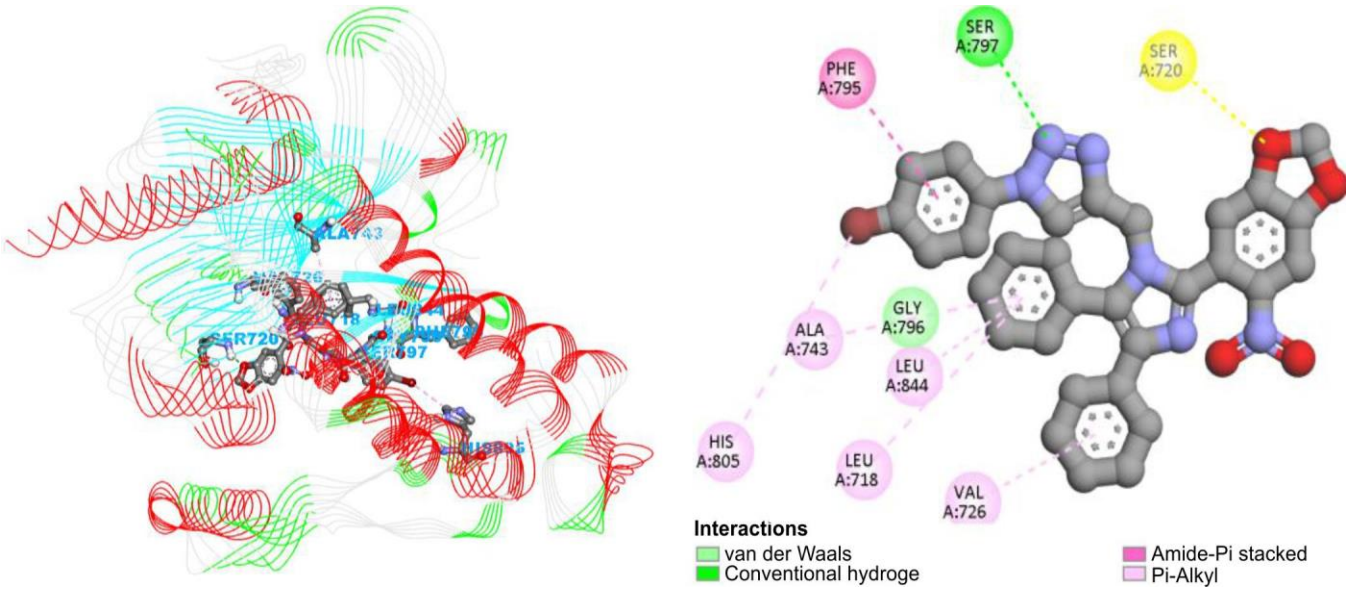

Fig. 2. 2D and 3D binding interactions of ligand **6f** against EGFR

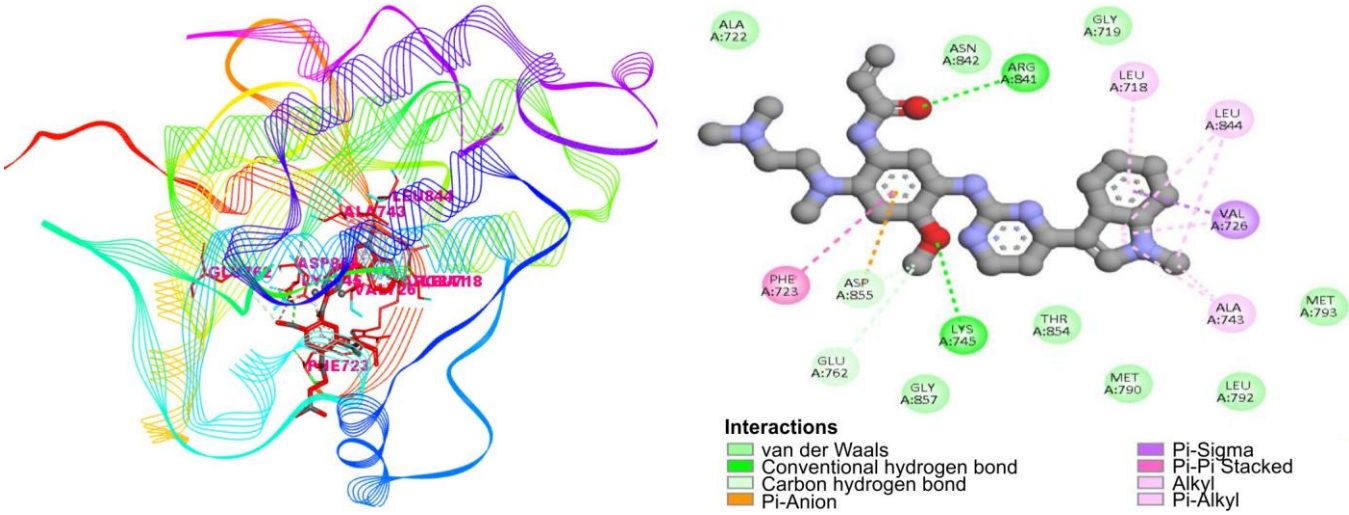

Fig. 3. 2D and 3D binding interactions of osimertinib against EGFR

TABLE-4
DOCKING SCORE AND BINDING
INTERACTIONS LIGANDS **6a-l** AGAINST EGFR

Compd.	Binding affinity (Kcal/mol)	Compd.	Binding affinity (Kcal/mol)
6a	-8.8	**6h**	-8.2
6b	-8.7	**6i**	-8.6
6c	-8.3	**6j**	-8.1
6d	-8.5	6K	-8.7
6e	-8.2	**6l**	-8.6
6f	-9.4	Osimertinib	-8.8
6g	-8.5		

Conclusion

A series of novel imidazole–triazole hybrid derivatives (**6a-l**) containing 6-nitrobenzo[*d*][1,3]dioxole moiety were successfully synthesised and characterised. The synthesised compounds exhibited promising anticancer activity against the MCF-7 cell line with comparatively lower toxicity toward NIH/3T3 normal cells. Among them, compound **6f** showed the highest cytotoxic activity and favourable selectivity profile. SAR analysis indicated that both electronic and steric effects of substituents significantly influence biological activity, with strong electron-withdrawing groups enhancing potency. The molecular docking studies revealed favourable binding interactions of the active compounds within the EGFR binding pocket, particularly for compound **6f**.

ACKNOWLEDGEMENTS

One of the authors, Potharaju Sunil Kumar, thanks to The Head, Department of Chemistry, Osmania University, Hyderabad for providing the laboratory facilities, CFRD, Osmania University for providing analytical support and UGC, New Delhi for the financial support.

CONFLICT OF INTEREST

The authors declare that there is no conflict of interests regarding the publication of this article.

DECLARATION OF AI-ASSISTED TECHNOLOGIES

During the preparation of this manuscript, the authors used an AI-assisted tool(s) to improve the language. The authors reviewed and edited the content and take full responsibility for the published work.

REFERENCES

1. E. Vitaku, D.T. Smith and J.T. Njardarson, *J. Med. Chem.*, **57**, 10257 (2014); https://doi.org/10.1021/jm501100b
2. M. Karnatak, P. Chak, D. Chaudhary and A. Kumar, *Mini-Rev. Med. Chem.*, (2026); https://doi.org/10.2174/0113895575438924260331114108
3. C. Jadala, S. Mishra, G.R. Potuganti, S. Cardoza and G.R. Velma, *RSC Adv.*, **16**, 21967 (2026); https://doi.org/10.1039/D6RA00737F
4. K.T. Jha, A. Shome, Chahat and P.A. Chawla, *Bioorg. Chem.*, **138**, 106680 (2023); https://doi.org/10.1016/j.bioorg.2023.106680
5. M.K. Kathiravan, A.B. Salake, A.S. Chothe, P.B. Dudhe, R.P. Watode, M.S. Mukta and S. Gadhwe, *Bioorg. Med. Chem.*, **20**, 5678 (2012); https://doi.org/10.1016/j.bmc.2012.04.045
6. J. Pérez-Villanueva, J.L. Medina-Franco, A. Hernández-Campos, T.R. Caulfield, F. Hernández-Luis, L. Yépez-Mulia and R. Castillo, *Eur. J. Med. Chem.*, **46**, 3499 (2011); https://doi.org/10.1016/j.ejmech.2011.05.016
7. B. Narasimhan, D. Sharma and P. Kumar, *Med. Chem. Res.*, **21**, 269 (2012); https://doi.org/10.1007/s00044-010-9533-9
8. S. Shalini, N. Kumar, S. Drabu and P. Sharma, *Beilstein J. Org. Chem.*, **7**, 668 (2011); https://doi.org/10.3762/bjoc.7.79
9. A. Kumar, P. Sharma and R. Kumari, *Eur. J. Med. Chem.*, **44**, 83 (2009); https://doi.org/10.1016/j.ejmech.2008.03.018
10. H.C. Kolb and K.B. Sharpless, *Drug Discov. Today*, **8**, 1128 (2003); https://doi.org/10.1016/S1359-6446(03)02933-7
11. V.D. Bock, H. Hiemstra and J.H. van Maarseveen, *Eur. J. Org. Chem.*, **2006**, 51 (2006); https://doi.org/10.1002/ejoc.200500483
12. D. Lengerli, K. Ibis, Y. Nural and E. Banoglu, *Expert Opin. Drug Discov.*, **17**, 1209 (2022); https://doi.org/10.1080/17460441.2022.2129613
13. A. Elkamhawy, N. Kim, A.H.E. Hassan, J. Park, J.-E. Yang, K.-S. Oh, B.H. Lee, M.Y. Lee, K.J. Shin, K.-T. Lee, W. Hur and E.J. Roh, *Eur. J. Med. Chem.*, **157**, 906 (2018); https://doi.org/10.1016/j.ejmech.2018.08.020

14. K. Nepali, S. Sharma, M. Sharma, P.M.S. Bedi and K.L. Dhar, *Eur. J. Med. Chem.*, **77**, 422 (2014); https://doi.org/10.1016/j.ejmech.2014.03.018
15. S. Morphy and Z. Rankovic, *J. Med. Chem.*, **48**, 6523 (2005); https://doi.org/10.1021/jm058225d
16. A.K. Jordão, V.F. Ferreira, T.M.L. Souza, G.G. de Souza Faria, V. Machado, J.L. Abrantes, M.C.B.V. de Souza and A.C. Cunha, *Bioorg. Med. Chem.*, **19**, 1860 (2011); https://doi.org/10.1016/j.bmc.2011.02.007
17. R. Kharb, P.C. Sharma and M.S. Yar, *J. Enzyme Inhib. Med. Chem.*, **26**, 1 (2011); https://doi.org/10.3109/14756360903524304
18. S. Kumar, B. Narasimhan and P. Sharma, *Eur. J. Med. Chem.*, **46**, 2816 (2011); https://doi.org/10.1016/j.ejmech.2011.04.002
19. P.P. Seth, C.R. Allerson, A. Berdeja and E.E. Swayze, *Bioorg. Med. Chem. Lett.*, **21**, 588 (2011); https://doi.org/10.1016/j.bmcl.2010.10.025
20. J. Cherkasov, E.N. Muratov, D. Fourches, A. Varnek, I.I. Baskin, M. Cronin, J. Dearden, P. Gramatica, Y.C. Martin, R. Todeschini, V. Consonni, V.E. Kuz'min, R. Cramer, R. Benigni, C. Yang, J. Rathman, L. Terfloth, J. Gasteiger, A. Richard and A. Tropsha, *J. Med. Chem.*, **57**, 4977 (2014); https://doi.org/10.1021/jm4004285
21. J. Bajorath, *Nat. Rev. Drug Discov.*, **1**, 882 (2002); https://doi.org/10.1038/nrd941
22. N. Patnam, K. Chevula, M. Srikanth, T. Jagadish, N. Nagaraju, S.R. Sagurthi and V. Manga, *ChemistrySelect*, **11**, e05698 (2026); https://doi.org/10.1002/slct.202505698
23. K. Chevula, P. Chennamsetti, N. Nagaraju, N. Patnam, S. Balabadra, P. Bhadraiah, I.R. Urma, K. Reddy and V. Manga, *Chem. Biodivers.*, **22**, e01142 (2025); https://doi.org/10.1002/cbdv.202501142